

Type-II Band Alignment and Enhanced Optical Properties in InP/Bi₂Se₃ van der Waals Heterojunctions: A First- Principles and FDTD Study

Xinhao Xu^a, Xin Guo^{a,b*}, Youchun Ma^{a,c*}, Aida Bao^a, Yayou Wang^a, Jie Wang^a,
Qianxi Jing^a, Yurou Li^b, Dongyu Yang^b, Yajun You^a, Yongpeng Zhao^{d*} and Pengfei
Shao^e

^a State key Laboratory of Extreme Environment Optoelectronic Dynamic Measurement
Technology and Instrument, North University of China, Taiyuan, 030051, People's
Republic of China

^b Shanxi Province Key Laboratory of Intelligent Detection Technology & Equipment,
North University of China, Shanxi, 030051, People's Republic of China

^c National Key Laboratory for Electronic Measurement Technology, North University
of China, Taiyuan 030051, People's Republic of China

^d College of Mechanical and Electrical Engineering, Sichuan Agricultural University,
Ya'an, 625000, People's Republic of China

^e Jiangsu Provincial Key Laboratory of Advanced Photonic and Electronic Materials,
School of Electronic Science and Engineering, Nanjing University, 163 Xianlin Road,
Nanjing, 210093, People's Republic of China

*E-mail: guoxin2019@nuc.edu.cn (X. Guo), mayouchun@nuc.edu.cn (Y. Ma),
zhaoy@sicau.edu.cn (Y. Zhao).

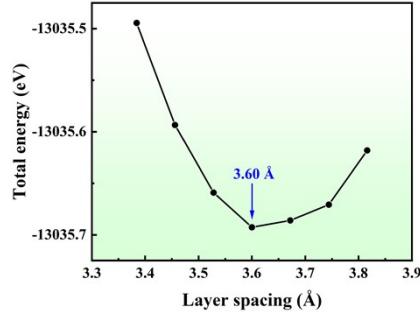


Figure S1 Binding energy curve analysis ($E_{\text{bind}}(d)$) for the H1 configuration, presented as the binding energy as a function of interlayer spacing.

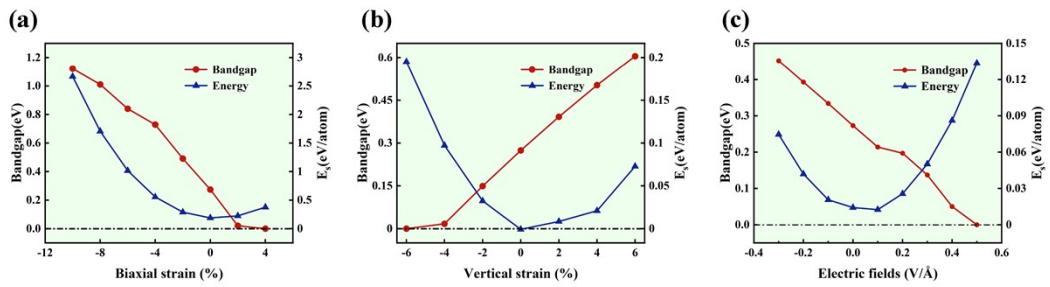


Figure S2 The influence of (a) biaxial strain, (b) vertical strain and (c) electric field on the bandgap and binding energy of the InP/Bi₂Se₃ vdWH.

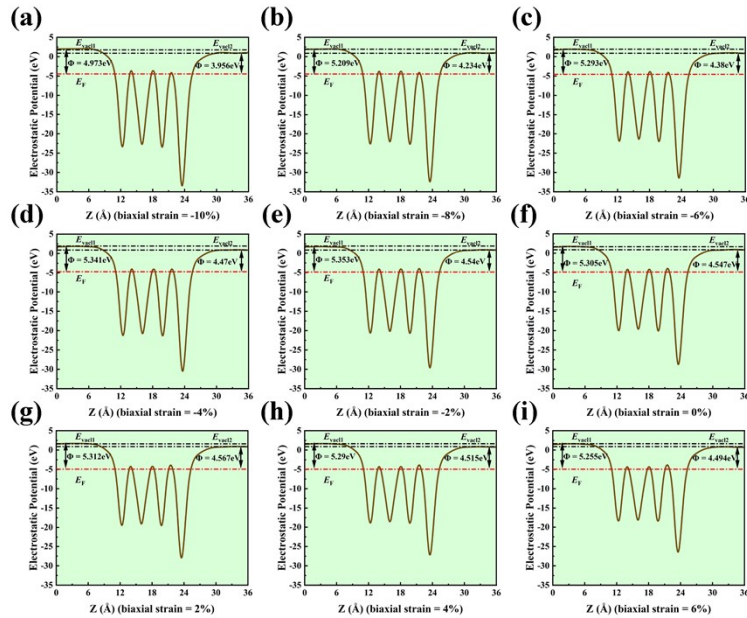


Figure S3 The variation of planar electrostatic potential and work function of the InP/Bi₂Se₃ vdWH under biaxial strain ranging from -10% to 6%. (The work function is marked on the corresponding graph.)

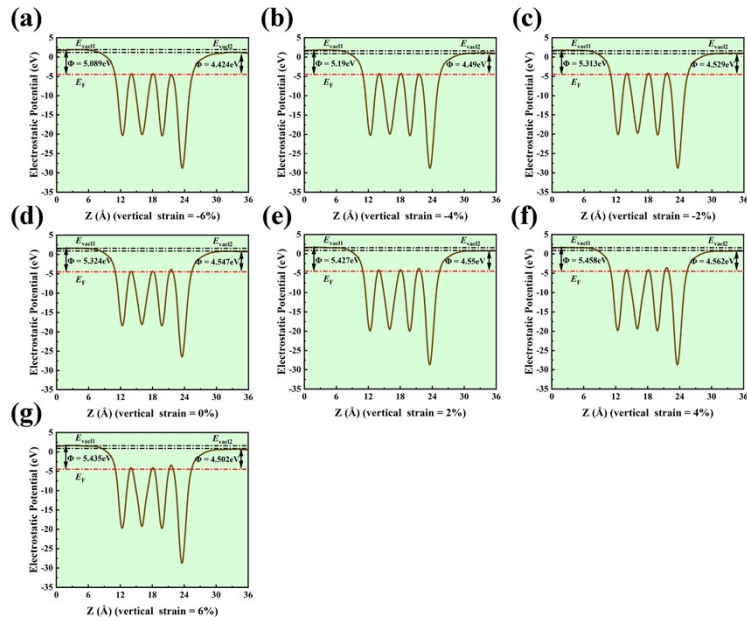


Figure S4 The variation of planar electrostatic potential and work function of the InP/Bi₂Se₃ vdWH under vertical strain ranging from -6% to 6%. (The work function is marked on the corresponding graph.)

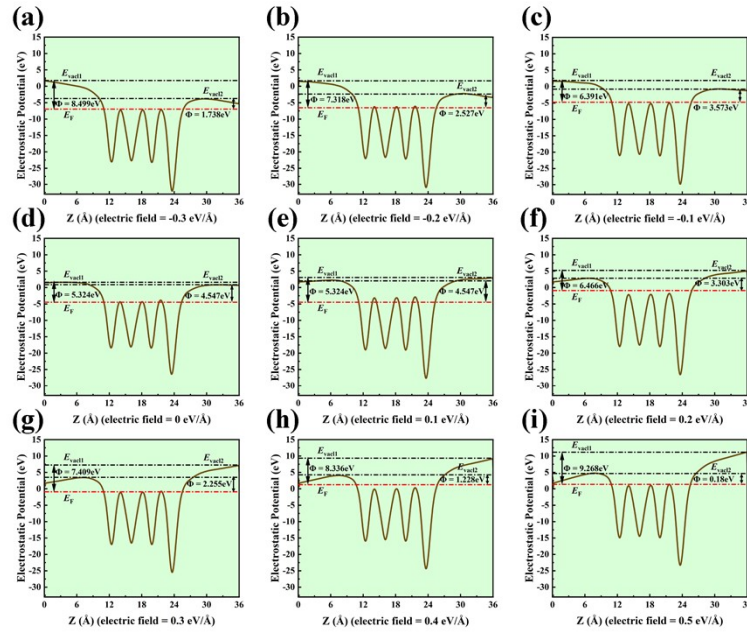


Figure S5 The variation of planar electrostatic potential and work function of the InP/Bi₂Se₃ vdWH under external electric fields ranging from -0.3 to 0.5 V/Å. (The work function is marked on the corresponding graph.)

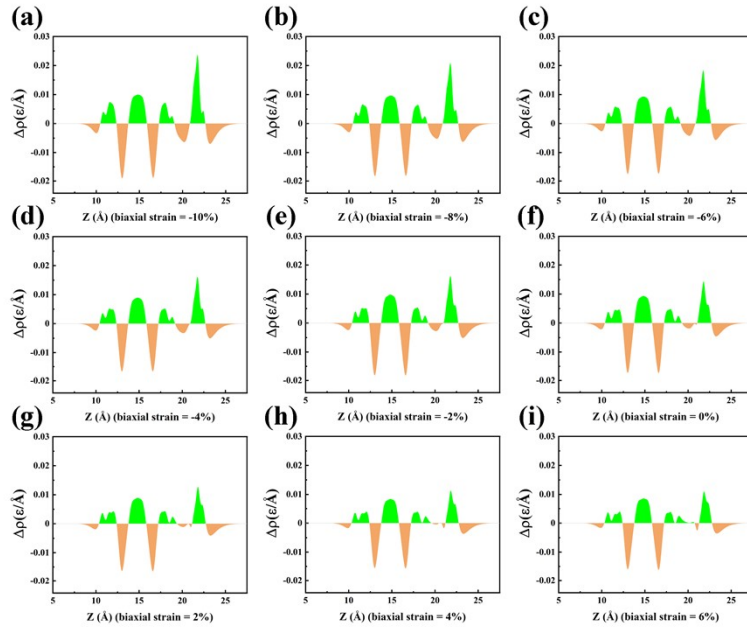


Figure S6 Differential charge density variation of the InP/Bi₂Se₃ vdWH under biaxial strain ranging from -10% to 6%.

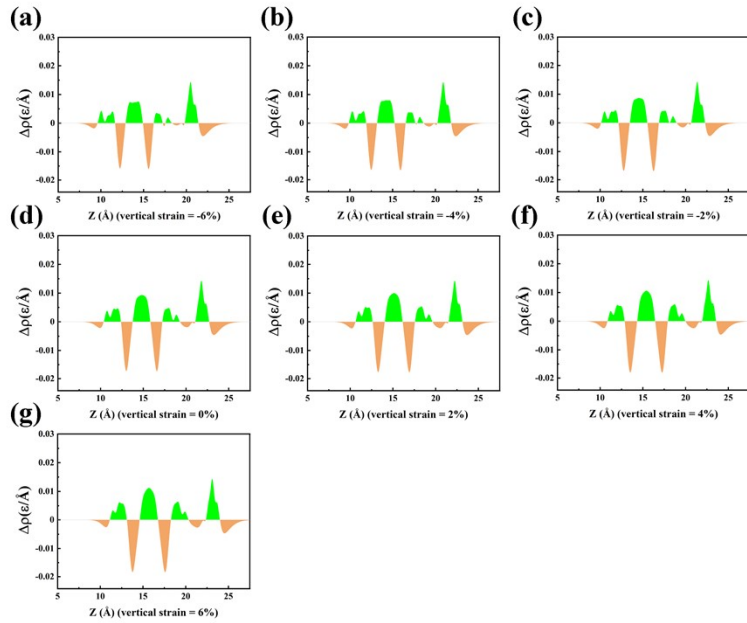


Figure S7 Differential charge density variation of the InP/Bi₂Se₃ vdWH under vertical strain ranging from -6% to 6%.

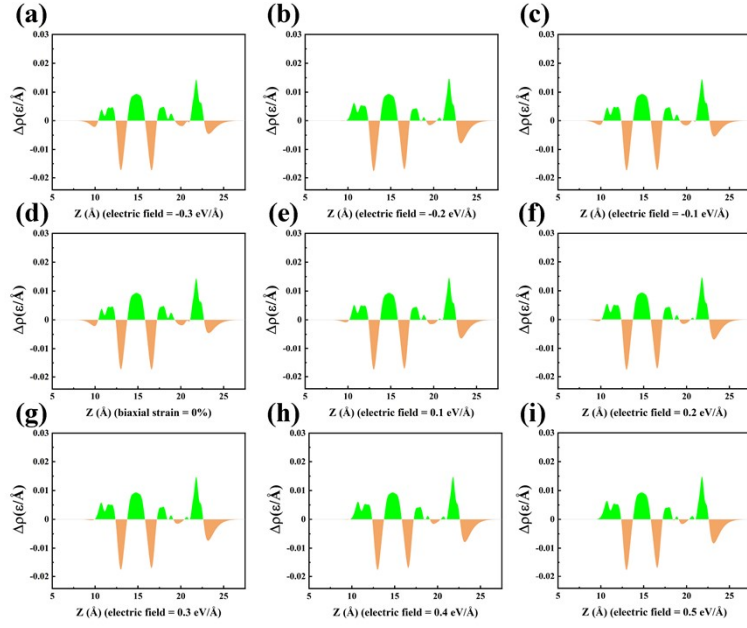


Figure S8 Differential charge density variation of the InP/Bi₂Se₃ vdWH under external electric fields ranging from -0.3 to 0.5 V/Å.

Table S1 Bader charge analysis of the InP/Bi₂Se₃ vdWH under different biaxial strains. Positive and negative values indicate electron accumulation and depletion, respectively.

Species	0.90	0.92	0.94	0.96	0.98	1	1.02	1.04	1.06
Bi	-1.01	-1.018	-1.03	-1.033	-1.03	-1.027	-1.021	-1.015	-1.008
Bi	-1.021	-1.031	-1.038	-1.036	-1.035	-1.033	-1.023	-1.02	-1.01
Se	0.621	0.625	0.627	0.628	0.627	0.625	0.626	0.623	0.62
Se	0.806	0.817	0.838	0.836	0.835	0.837	0.829	0.682	0.829
Se	0.619	0.622	0.623	0.623	0.621	0.618	0.614	0.61	0.603
In	-0.712	-0.749	-0.798	-0.793	-0.805	-0.811	-0.811	-0.806	-0.794
P	0.697	0.734	0.778	0.776	0.787	0.79	0.786	0.776	0.761

Table S2 Bader charge analysis of the InP/Bi₂Se₃ vdWH under different vertical strains. Positive and negative values indicate electron accumulation and depletion, respectively.

Species	0.94	0.96	0.98	1	1.02	1.04	1.06
Bi	-1.04	-1.038	-1.032	-1.028	-1.021	-1.016	-1.011
Bi	-1.046	-1.042	-1.038	-1.033	-1.027	-1.021	-1.011

